Studies of adsorbed monolayers using a spatially coupled Potts model

1989 J. Phys. A: Math. Gen. 22 3011

(http://iopscience.iop.org/0305-4470/22/15/017)

J. Phys. A: Math. Gen. 22 (1989) 3011–3021. Printed in the UK

Studies of adsorbed monolayers using a spatially coupled Potts model

M P Allen and K Armitstead
H H Wills Physics Laboratory, University of Bristol, Royal Fort, Tyndall Avenue, Bristol BS8 1TL, UK

Received 31 March 1989

Abstract. We present a study of a model proposed by Sluckin to represent molecular monolayers adsorbed on a surface. Monte Carlo simulations and a Müller-Hartmann–Zittartz interface free energy calculation reveal that the region of stability of the low-temperature herringbone phase of this system is much less extensive than was originally thought. The analysis indicates that the model exhibits a very rich phase diagram, which merits further investigation.

1. Introduction

In this paper we investigate the phase diagram of an orientationally dependent Potts-type model, recently introduced by Sluckin [1] to describe the 'herringbone phase', which is observed experimentally in nitrogen adsorbed on graphite [2,3] . In this two-dimensional (monolayer) phase the molecules form a triangular lattice in registry with the substrate, and preferentially align along the crystal axes. The particular arrangement known as the herringbone phase is shown in figure 1, labelled 'HB'. This phase is also observed in many other systems, such as hydrogen at low temperatures [4] and smectic-E liquid crystals [5,6], hence a general Hamiltonian which describes the common physical features of these structures would be very useful. We examine both numerically and analytically such a proposed Hamiltonian [1] to determine its physical applicability, and discover indications of a rich phase diagram. Its properties include multiphase points, various types of domain wall and wetting lines — all of which have received considerable attention in recent literature [7,8] and may warrant further study.

The layout of this paper is as follows. Section 2 describes the model and summarises the results already obtained. Section 3 describes and reports the results from a Monte Carlo study performed on a distributed array processor (DAP). In §4 we present an analysis of the interfacial behaviour and use approximate techniques to locate the position of the phase boundaries. Finally, §5 contains a discussion and suggests future areas of study.

2. The model

The model is defined by the Hamiltonian [1]

$$\mathcal{H} = \sum_{<ij>} J_1 \delta_{s_i s_j} \delta_{s_i r_{ij}} \delta_{s_j r_{ij}} + J_2 (1 - \delta_{s_i r_{ij}})(1 - \delta_{s_j r_{ij}}) \delta_{s_i s_j} \tag{1}$$

0305-4470/89/153011+11$02.50

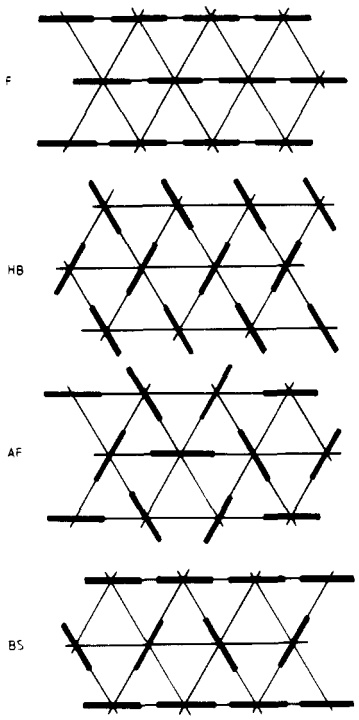

Figure 1. The ground-state configurations: ferromagnetic (F), $E_{gs} = J_1 + 2J_2$; herringbone (HB), $E_{gs} = J_2$; antiferromagnetic (AF), $E_{gs} = 0$; blanket-stitch (BS), $E_{gs} = J_1/2$.

where $< ij >$ denotes that the sum is to be taken over all pairs of nearest-neighbour sites i and j, located on a triangular lattice, s_i is a three-state spin which can have an alignment along one of the three lattice axes, and r_{ij} labels the lattice axis to which the vector joining i and j belongs. As for the standard Potts model, only neighbouring spins which are in the same state have a non-zero energy; in the case studied here, however, the coupling of the spin directions to the lattice vectors introduces an asymmetry into the interaction parameters. Parallel spins aligned along the lattice vector joining them have an interaction energy of J_1, whilst all other parallel spins interact with energy J_2. This information is displayed diagramatically in figure 2.

The ground state of the model for a particular choice of J_1 and J_2 may be found by minimising the total energy per spin, E_{gs}. Careful counting of all possible arrangements leads to four ground-state configurations: ferromagnetic (F), $E_{gs} = J_1 + 2J_2$; herringbone (HB), $E_{gs} = J_2$; antiferromagnetic (AF), $E_{gs} = 0$; blanket-stitch (BS), $E_{gs} = J_1/2$. These configurations are sketched in figure 1. The regions of stability of these phases are shown in figure 3.

It is convenient to parametrise J_1 and J_2 as

$$J_1 = J(1-\alpha) \qquad J_2 = -J\alpha \tag{2}$$

and to define a reduced temperature $k_B T/J$ where k_B is Boltzmann's constant. This paper focuses on the HB and F phases, which are of most obvious physical interest. This corresponds to $J_1 > 0$ and $J_2 < 0$, i.e. $0 \leq \alpha \leq 1$ and $J > 0$. This region is shaded in figure 3. At $T = 0$ the HB and F phases meet in a multiphase point at $\alpha = \frac{1}{2}$. A

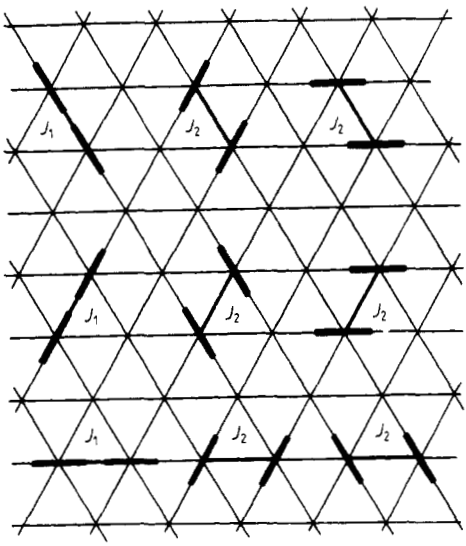

Figure 2. The arrangements of neighbouring spins which have a non-zero interaction energy.

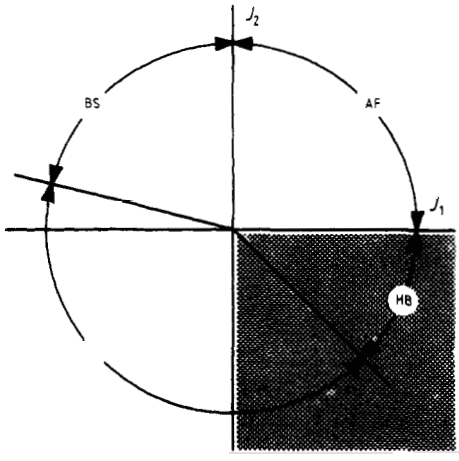

Figure 3. Regions of stability for different ground states. The region under study here is shaded.

second multiphase point divides HB and AF phases at $\alpha = 0$. For sufficiently high T, at any α, the disordered phase will be stable; consequently, as the temperature is lowered, we expect to see a transition to one or other of the ordered phases.

The phase diagram obtained by Sluckin [1] via mean-field theory is shown in figure 4. Due to the neglect of fluctuations inherent in such a theory this should provide an upper limit for the boundaries. Sluckin also used a Müller-Hartmann–Zittartz (MHZ) method [9] for the interface free energy to find the position of the phase boundaries. We have recalculated his results, making some amendments, and compare with our own work using this method in §4.

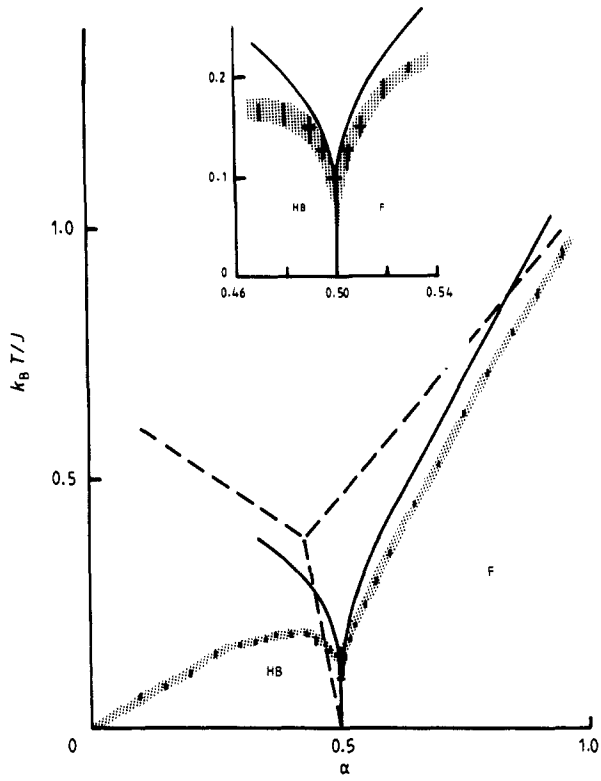

Figure 4. The phase diagram from mean-field theory [1] (broken curve); as predicted by our analysis (full curve); and from our Monte Carlo simulations (shaded). We show transition points determined from sequences of runs at constant α (vertical bars) and at constant T (horizontal bars). The estimated error is represented by the length of the bar in each case. Inset: the region around $\alpha = 0.5$.

3. Monte Carlo simulations

We carried out Monte Carlo simulations on a parallel processing computer, the DAP 510. This consists of a 32×32 array of processors, operating in concert. Many of the technical details of Monte Carlo simulations performed on this machine have been published before [10,11], so we just give a brief summary here.

Our system consisted of 4096 spins arranged in a 64×64 rhombus with periodic boundary conditions, on a triangular lattice (each spin having six nearest neighbours). The spins were treated as lying on four interpenetrating 32×32 sublattices; all the three-state spin values belonging to a given sublattice were stored in a single DAP 'matrix' variable. The nearest-neighbour character of the interactions meant that the usual Monte Carlo updating scheme could be applied to all spins in a given sublattice simultaneously and independently; herein lies the parallelism of the technique.

The DAP is very efficient at manipulating logical variables and small integers, and at performing the shifting operations necessary to compute some of the nearest-neighbour interactions. Also, the two-dimensional periodic boundary conditions are built into the hardware. The program was written in a parallel extension of FORTRAN and ran at about 60 MC sweeps per second (1 sweep = 1 attempted flip per spin), i.e. nearly

0.25×10^6 spin flips per second.

We used a standard Metropolis Monte Carlo algorithm [12], attempting to randomly change the state of each spin for each sublattice in turn. Cooling sequences of runs with fixed parameter α were initiated from a random initial configuration, and continued thereafter at steadily decreasing temperatures, the final configuration for one run being used as the initial configuration for the next. Complementary heating sequences were initiated from completely ordered herringbone or ferromagnetic configurations, for $\alpha < \frac{1}{2}$ and $\alpha > \frac{1}{2}$ respectively. Typical runs were of length 10 000 sweeps, of which 3000 were discarded to allow time for equilibration. The temperatures $k_B T/J$ between successive runs typically differed by 0.02 units. In the most interesting region of the phase diagram, $\alpha \simeq \frac{1}{2}$, longer runs of 30 000 sweeps (discarding 10 000) were employed, and the temperature incremented in units of 0.005. Some sequences in this region were undertaken at constant temperature, changing the α parameter in units of 0.001, and using still longer runs of 60 000 sweeps (discarding 20 000). In all, about 1000 state points were simulated. This survey would have been very time-consuming on anything other than a supercomputer or special-purpose machine.

We observed order–disorder phase transitions which were located by monitoring the appropriate herringbone and ferromagnetic order parameters, defined by summing the spins in the correct orientations for a given ground state, and maximising with respect to the various degenerate choices of ground state. On comparing heating and cooling sequences, some evidence of hysteresis was seen around the phase transition. However, for most values of α, the hysteresis extended only over a single step in temperature, and we consider that our runs are long enough, and sufficiently closely spaced, to locate the transition points quite accurately. Well defined jumps in the order parameter were seen in most cases. We have made no serious attempt to determine the order of the transition, and its dependence on the parameters, as yet. In the most difficult region, $\alpha = 0.50 \pm 0.01$, where the transition temperature was quite low, ($k_B T/J < 0.1$) the system behaved in a sluggish manner, and values of the order parameter were less reproducible. Nonetheless, the transition temperatures could still be determined quite well, and good agreement was obtained between temperature sweeps at constant α and sweeps in α at constant temperature. The transition points determined from these simulations are shown in figure 4. The error bars are estimated from the extent of hysteresis seen in each case. In the inset we expand the interesting region around the $T = 0$ HB/F boundary, $\alpha = \frac{1}{2}$.

4. Interfacial analysis

In this section we make a preliminary calculation of the position of the phase boundaries using the method of Müller-Hartmann and Zittartz [9] to estimate the interfacial free energy between two degenerate phases. At the phase boundary this free energy vanishes, hence a value for the critical temperature may be obtained. An interface is introduced into the system by a suitable choice of boundary conditions — altering the boundary conditions may give a different interface and associated free energy, even at zero temperature. Therefore we begin with an analysis of the interfaces which occur at $T = 0$, before calculating the free energy of those which are energetically favourable.

4.1. Interfaces at zero temperature

We consider a rhombic triangular lattice with fixed boundary conditions in the top

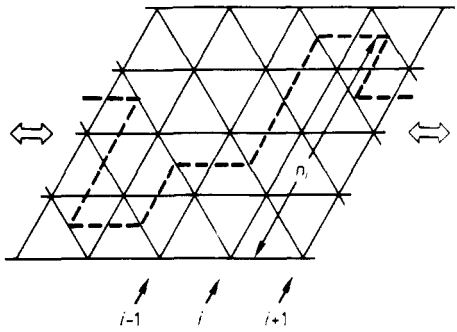

Figure 5. The geometry of the triangular lattice. The broken line shows an interface passing through the system. i labels diagonal columns as explained in §4.2 and n_i is the height of the ith column. The double-headed arrows indicate that periodic boundary conditions apply. The top and bottom rows of spins are fixed in the appropriate orientations.

and bottom rows and periodic boundary conditions in the other lattice directions, as shown in figure 5.

In the F phase, $\frac{1}{2} < \alpha$, which is threefold degenerate, there are six possible choices of boundary conditions giving rise to an interface in the system. However, only two are symmetrically distinct, and these are are shown in figure 6. The corresponding energies are (i) $E_0 = (2\alpha - 1)NJ$ and (ii) $E_0 = (2\alpha - \frac{1}{2})NJ$, where N is the length of the interface in lattice spacings. The first of these is the more stable for all α, and therefore we use this set of boundary conditions in the next section.

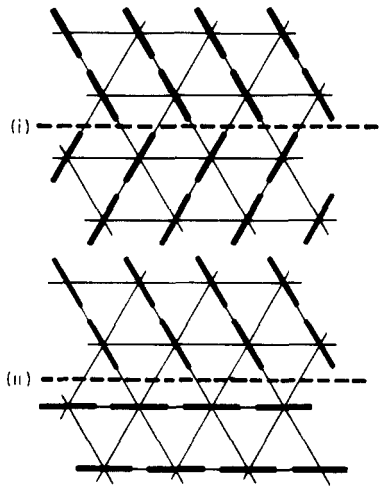

Figure 6. The two distinct interfaces in the F phase. Associated ground-state energies are: (i) $E_0 = (2\alpha - 1)NJ$; (ii) $E_0 = (2\alpha - \frac{1}{2})NJ$. N is the length of the interface in lattice spacings.

In the HB phase, $0 < \alpha < \frac{1}{2}$, the ground state is sixfold degenerate and there are many possible different interfaces. Figure 7 shows the interfaces which have the lowest energy for various ranges of α.

For $0.4 < \alpha < 0.5$, the interface labelled (i) in figure 7 has the lowest energy, $E_0 = (1 - 2\alpha)NJ$. Notice that this energy is unaffected by any vertical displacement of

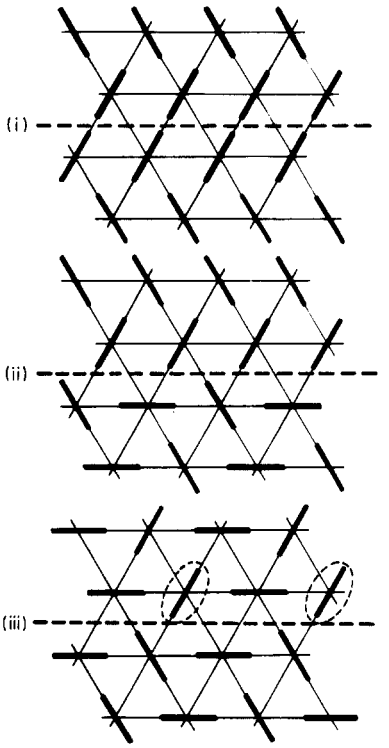

Figure 7. The interfaces in the HB phase which have the lowest energy E_0, in the following ranges of α: (i) $0.4 < \alpha < 0.5$, $E_0 = (1 - 2\alpha)NJ$; (ii) $0 < \alpha < 0.4$, $E_0 = \frac{1}{2}\alpha NJ$; (iii) $0 < \alpha < 0.4$, $E_0 = \frac{1}{2}\alpha NJ$. N is the length of the interface in lattice spacings. In case (iii), the circled spins can flip from / to \ at zero energy cost.

that interface.

For $0 < \alpha < 0.4$ there are two non-equivalent interfaces, (ii) and (iii), with the same lowest energy $E_0 = \frac{1}{2}\alpha NJ$. Only alternate vertical translations of (ii) give this energy; translating upward by one lattice spacing (or equivalently reversing the phase of the upper herringbone structure) gives a higher energy $E_0 = \frac{1}{2}(1 - \alpha)NJ$. Entropic fluctuations of (ii) at non-zero temperatures will therefore be reduced compared with, say, those of (i). Interface (iii) is particularly interesting because it has a finite entropy at $T = 0$. The circled spins can flip from / to \ at zero energy cost giving an entropic contribution $\frac{1}{2}Nk_B \ln 2$ to the interface free energy, and therefore (iii) will always be preferred to (ii).

For $\frac{1}{3} < \alpha < 0.4$, a type-(i) herringbone interface may occur in the system with suitable boundary conditions, although it will not be a minimum energy interface as shown above. However, for $\alpha < \frac{1}{3}$, type-(iii) or type-(ii) interfaces of total length $2N$ are energetically preferable to one type-(i) interface of length N. Some consideration of figure 7 reveals that it is not possible for a type-(i) interface to transform into type-(iii) interfaces without producing an interface of length much larger than $2N$. It may, however, split into two type-(ii) interfaces with an arbitrary even number of layers of a third phase intervening. This leads to the possibility of a wetting transition at non-zero temperature.

We now use these conclusions to study the phase diagram for $T > 0$.

4.2. Non-zero temperatures

The free energy associated with an interface between two degenerate phases involves evaluating the partition function over all possible fluctuations of the interface and the surrounding bulk phases. This, in general, is not feasible and some approximation must be made. The approach we shall use here, due to Müller-Hartmann and Zittartz (MHZ) [9], divides the system into a series of columns and completely determines an arbitrary interface configuration by the single-valued height at which it passes through the set of columns, $\{n_i\}$. Therefore all overhangs of the interface and bulk excitations are neglected; however, the sum over remaining configurations may be readily evaluated. We emphasise that this particularly simplistic model must not be taken as an accurate prediction but rather used in conjunction with MC results as an indication of interesting aspects of the phase diagram which warrant a more thorough investigation.

Following the notation of [9], the interface free energy per column is given by

$$\sigma = E_0 - k_B T \lim_{N\to\infty} \frac{1}{N} \ln Z \tag{3}$$

where E_0 is the ground-state energy per column of the flat interface, N is the number of columns, Z is the interface partition function

$$Z = \sum_{\{n_i\}} \exp(-\Delta E\{n_i\}/k_B T) \tag{4}$$

and $\Delta E\{n_i\}$ is the interface energy associated with configuration $\{n_i\}$ compared with the reference system. For a triangular lattice we choose our columns to be directed along one of the diagonal lattice axes, as shown in figure 5. This is equivalent to the fluctuations included by Southern [13] for the Ising model, and which give agreement with exact results. It differs from the subset chosen by Sluckin [1]; however, it automatically includes all of his configurations and avoids problems (overlooked in his work) with applying periodic interfacial boundary conditions. It should also be noticed that his 'step energy' in the F region of $(\alpha - \frac{1}{2})J$ is incorrect and should be αJ; we include his amended results in figure 8 for comparison.

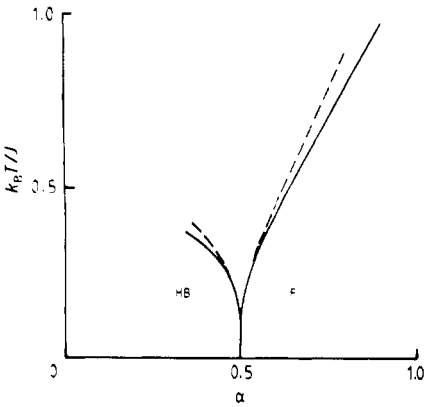

Figure 8. The phase diagram from the corrected MHZ analysis of Sluckin [1] (broken curve), and from our MHZ analysis (full curve).

In the F region, using the the first interface in figure 6 as our reference system, the value of $\Delta E\{n_i\}$ for an arbitrary interface configuration is given by

$$\Delta E\{n_i\} = \sum_{i=1}^{N} |n_{i+1} - n_i| J\alpha \qquad -\infty \leq n_i \leq \infty. \tag{5}$$

The partition function for all such fluctuations, as defined by equation (4) may readily be evaluated as

$$Z = \left(\frac{1 + \exp(-\alpha J/k_B T)}{1 - \exp(-\alpha J/k_B T)}\right)^N. \tag{6}$$

This leads to an expression for the total interface free energy:

$$\sigma = (2\alpha - 1)J - k_B T \ln\left(\frac{1 + \exp(-\alpha J/k_B T)}{1 - \exp(-\alpha J/k_B T)}\right). \tag{7}$$

Setting $\sigma = 0$ determines the phase boundary. This is compared with the mean-field prediction and with our Monte Carlo results in figure 4. We compare with Sluckin's analysis in figure 8. As anticipated, the inclusion of more fluctuations in our method moves the phase boundary to lower temperatures. Reasonable agreement with the MC results is apparent.

In the HB phase, the expression for $\Delta E\{n_i\}$ for a type-(i) interface (see figure 7) is also given by equation (5). Hence the interfacial tension is given by

$$\sigma = (1 - 2\alpha)J - k_B T \ln\left(\frac{1 + \exp(-\alpha J/k_B T)}{1 - \exp(-\alpha J/k_B T)}\right). \tag{8}$$

We have plotted the resulting phase boundary for $0.4 < \alpha < 0.5$ in figure 4, for comparison with mean-field and Monte Carlo results, and again compare with Sluckin's analysis in figure 8. It is clear that the difference between theory and simulation grows significantly as α falls to 0.4. The discrepancy would continue to grow if the curve were extended to lower α, but as we have seen this would be incorrect even in principle, since a lower-energy ground-state interface appears for $\alpha < 0.4$.

For $0 < \alpha < 0.4$ the evaluation of the type-(iii) interface partition function is non-trivial because $\Delta E\{n_i\}$ depends on the actual values of n_i as well as their differences. However, all elementary excitations have an energy proportional to αJ, so the low-temperature interface free energy may be expected to take the form

$$\sigma = \tfrac{1}{2}\alpha J - \tfrac{1}{2}k_B T \ln 2 - k_B T f(\alpha J/k_B T) \tag{9}$$

where the first term is the $T = 0$ energy, the second is temperature multiplied by the ground-state entropy and the final term is due to fluctuations. The phase boundary will therefore have the form $k_B T/\alpha J$ = constant, which is consistent with the Monte Carlo results.

Finally, we consider the possibility of a wetting transition for $T > 0$ in the vicinity of $\alpha = \frac{1}{3}$. A calculation of the surface tension of a herringbone type-(ii) interface using a MHZ method as above could be used to predict whether wetting would occur via the condition

$$2\sigma(\text{type-(ii)}) = \sigma(\text{type-(i)}).$$

However, this is significantly more complicated than the above calculations because the step energy no longer depends solely on the step height. We return to this in the following section.

5. Discussion

In this paper, we have re-examined and extended the work of Sluckin on the stability of herringbone and ferromagnetic phases for this model, and have compared with computer simulation results. The incorporation of a larger set of fluctuations into the Müller-Hartmann–Zittartz treatment [9] slightly improves (i.e. lowers) the upper bounds on the transition temperatures in each case. For the ferromagnetic case the MHZ approach predicts the phase boundary quite well. However, away from the multiphase point at $\alpha = \frac{1}{2}$, it greatly overestimates the range of stability of the herringbone phase.

This failure of the MHZ method is not surprising. For some models which have only two degenerate low-temperature phases, such as the Ising model on square and triangular lattices [13,14] the method gives very good agreement with exact calculations. However, for two-state models in general it is not possible to judge in advance the probable accuracy of a calculation nor the optimal interface orientation, although Lin and Wu [15] have discussed conditions which should be met to obtain any degree of accuracy. For models with several degenerate ground states, as here, the restriction to a single-valued interface profile may cause the method to fail, because many phases which could appear at the interface are automatically excluded. Various multistate models have been studied by Selke and Yeomans [16] using a modified MHZ method which allows for non-boundary states to be adsorbed at the interface. Their results show that neglect of the adsorbed states will always lead to an overestimate of the phase transition temperature, and that if a wetting transition occurs then inclusion of the surface-adsorbed state is vital to obtaining even qualitatively correct results.

We have examined the interface structures generated by our Monte Carlo simulations specifically to test this point. For the ferromagnetic interfaces of figure 6, very little surface adsorption seems to occur, right up to the transition temperature, and this is consistent with the agreement obtained between the MHZ theory and the simulation results shown in figure 4. On the herringbone side, however, for $0.4 < \alpha < 0.5$, we see significant adsorption of additional phases at the interface (type (i) in figure 7). This will invalidate the calculation of the interfacial tension, equation (8), and lead to inaccurate transition temperatures, as we see in figure 4. The extension of the theory to $\alpha < 0.4$ requires the explicit evaluation of column-to-column transfer matrices for type-(ii) and type-(iii) interfaces. However, the degeneracy of the interfaces with respect to lattice directions leads to infinite eigenvalues which cannot be sensibly removed. Therefore the MHZ method completely fails in these cases. An alternative approach for locating the phase boundaries would be the use of finite-size scaling [17], to extrapolate from exact small-system results to the thermodynamic limit. In practice, this is expensive in terms of computer time, for this model.

Similar comments apply to the investigation of a possible wetting transition in the herringbone phase around $\alpha = \frac{1}{3}$. Ideally we should allow for an intervening third phase of arbitrary thickness at a type-(i) interface (see figure 7), and determine the lowest surface free energy as a function of the thickness. This would be non-trivial, and preliminary investigations are underway. The low entropic contributions in a type-(ii) interface means that we cannot prejudge whether a wetting transition occurs.

However, the vast overestimation of the phase transition temperatures by the MHZ method compared with the MC results, and our own observations of surface adsorption in MC simulations of the interface, suggest that this is a significant factor.

Our results indicate that, for this discrete-state model, the herringbone phase is highly vulnerable to fluctuation effects, which ultimately produce the disordered phase. We may expect this to be even more the case for continuous spin models. In particular, it will be interesting to fully characterise the phase transition in the discrete case and compare with the anisotropic planar rotor model (see [18] and references therein), in which a fluctuation-induced first-order transition occurs. Also, the possibility exists of extending the simulation and analysis to include vacant sites and/or spin states representing vertically oriented molecules. This work is currently in progress.

Acknowledgments

It is a pleasure to thank Tim Sluckin for providing a preprint of [1] and for helpful conversations, particularly in relation to the $\alpha = 0$ limit. The DAP was provided under the Computational Science Initiative of the SERC, and we made use of fast video output facilities provided on loan by Active Memory Technology. One of us (KA) is an SERC Research Fellow.

References

[1] Sluckin T J 1988 *J. Phys. A: Math. Gen.* **21** 1415
[2] Chung T T and Dash J G 1977 *Surf. Sci.* **66** 559
[3] Diehl R D, Toney M F and Fain S C Jr 1982 *Phys. Rev. Lett.* **48** 177
[4] Harris A B and Berlinsky A J 1979 *Can. J. Phys.* **57** 1852
[5] Meyer R J 1975 *Phys. Rev.* A **12** 1066
[6] Meyer R J 1976 *Phys. Rev.* A **13** 1613
[7] Huse D A and Fisher M E 1982 *Phys. Rev. Lett.* **49** 793
[8] Dietrich S 1988 *Phase Transitions and Critical Phenomena* vol 12 ed C Domb and J Lebowitz (New York: Academic) p 1
[9] Müller-Hartmann E and Zittartz J 1977 *Z. Phys.* B **27** 261
[10] Fincham D 1987 *Molecular Simulation* **1** 1
[11] Allen M P and O'Shea S F 1987 *Molecular Simulation* **1** 47
[12] Metropolis N, Rosenbluth A W, Rosenbluth M N, Teller A H and Teller E 1953 *J. Chem. Phys.* **21** 1087
[13] Southern B W 1978 *Z. Phys.* B **30** 61
[14] Burkhardt T W 1978 *Z. Phys.* B **29** 129
[15] Lin K Y and Wu F Y 1979 *Z. Phys.* B **33** 181
[16] Selke W and Yeomans J M 1983 *J. Phys. A: Math. Gen.* **16** 2789
[17] Duxbury P M, Yeomans J M and Beale P D 1984 *J. Phys. A: Math. Gen.* **17** L179
[18] Mouritsen O G 1984 *Computer studies of phase transitions and critical phenomena* (Berlin: Springer) ch 5